Singularities in twist-3 quark distributions

Fatma P. Aslan and Matthias Burkardt
Department of Physics, New Mexico State University, Las Cruces, New Mexico 88003-0001, USA

(Received 14 March 2019; published 13 January 2020)

We find in one-loop calculations and spectator models that twist-3 generalized parton distributions exhibit discontinuities. In the forward limit, these discontinuities grow into Dirac delta functions which are essential to satisfy the sum rules involving twist-3 parton distribution functions (PDFs). We calculate twist-3 quasi-PDFs as a function of longitudinal momentum and identify the Dirac delta function terms with momentum components in the nucleon state that do not scale as the nucleon is boosted to the infinite momentum frame.

DOI: 10.1103/PhysRevD.101.016010

I. INTRODUCTION

A complementary picture of the nucleon structure is obtained by simultaneous information on both transverse spatial and longitudinal momentum distributions of partons. The relevant physical observables are generalized parton distributions (GPDs) [1–4]. Theoretically, they are calculated from nonforward matrix elements of nonlocal operators, and experimentally, they are accessible through exclusive deep inelastic scattering experiments, such as deeply virtual Compton scattering (DVCS) [4,5]. GPDs give information about the spin, momentum, and spatial distribution of the quarks, antiquarks, and gluons within a fast moving nucleon [6–8] and, therefore, provide a remarkable insight on its inner structure.

One property to classify the GPDs is their twist [9]. Twist determines the order in Q^2 (squared four-momentum transfer) at which a matrix element contributes to the physical amplitude of a given hard process. With increasing twist, the number of partons which participate in that matrix element also tend to increase. At leading twist, twist-2, GPDs describe two-particle correlations in the nucleon, while the next leading twist, twist-3, GPDs also involve three-particle correlations, such as quark-gluon-quark (qgq). It is advantageous to define the twist in the infinite momentum frame (IMF) where the nucleon has a large momentum in the longitudinal direction (direction of the nucleon propagation), i.e., $P^+ \gg M$, and nearly zero momentum in the transverse direction, i.e., $P_T \approx 0$ [10]. In the IMF, the twist of a distribution can be identified with its behavior under a longitudinal momentum boost. While twist-2 distributions are invariant under the boosts along the longitudinal direction, twist-3 distributions change as $1/P^+$.

In the Bjorken limit, the matrix elements are dominated by twist-2 operators [11]. Even though they are mostly relevant for subleading corrections, there are several motivations to study twist-3 GPDs. For example:

(i) They involve a novel type of information on qgq correlations which is not contained in twist-2 distributions. These qgq correlations can be interpreted as an average transverse color Lorentz force acting on the quarks inside a nucleon [12]. The new information embodied in twist-3 GPDs is the distribution of that force on the transverse plane.

(ii) At low Q^2, the twist-3 contamination can be significant. Therefore, twist-3 corrections may not be negligible in the upcoming detailed measurements of DVCS amplitude at 12 GeV in Jefferson Lab. On the other hand, it has been shown that in the analysis of DVCS amplitude, the electromagnetic gauge invariance requires twist-3 contributions in the asymptotic regime [13,14].

(iii) Twist-3 GPDs may provide an alternative source of information on orbital angular momentum of the quarks through the sum rule which relates the second moment of a particular twist-3 GPD, G_2, and kinetic angular momentum of the quarks inside a longitudinally polarized nucleon [15–17],

$$L^q_{\rm kin} = -\int dx x G^q_2(x, \xi = 0, t = 0), \qquad (1)$$

where x is the average longitudinal quark momentum, ξ is the longitudinal, and t is the total momentum transfer to the nucleon.

Twist-3 GPDs generically exhibit discontinuities at the points of particular interest and importance ($x = \pm\xi$). These points correspond to configurations in which one of the partons has a vanishing momentum component in the matrix element describing the scattering amplitude. There are several studies [17–30] which reveal the discontinuties of twist-3 GPDs using Wandzura-Wilczek (WW) approximation [31]. However, we show that twist-3 GPDs are also discontinuous in the quark target model (QTM) and scalar diquark model (SDM) without using WW approximation. Potentially the discontinuities lead to divergent scattering amplitudes and endanger the factorization of the hard-scattering process [32]. However, in Ref. [33] it has been shown that the discontinuities cancel for the linear combinations of twist-3 GPDs which enter the DVCS amplitude, and therefore, twist-3 amplitudes are consistent with DVCS factorization. Even though they do not exhibit a problem for factorization, we will show that in the forward limit the discontinuities can grow into Dirac delta functions which are essential for satisfying relevant Lorentz invariance relations. Investigating twist-3 quasi-PDFs (parton distribution functions) as a function of the longitudinal momentum reveals that the Dirac delta function terms correspond to momentum components in the nucleon state that do not scale as the nucleon is boosted to the IMF.

There are several parametrizations of the correlators which define GPDs [25,27,34]. The relations between the different parametrizations are given in Ref. [33]. We use the following parametrization [28] and adopt the light front gauge $A^+ = 0$ where the Wilson lines can be ignored [35]:

$$\frac{1}{2}\int\frac{dz^-}{2\pi}e^{ixp^+z^-}\langle P',S'|\bar{q}\left(-\frac{z^-}{2}\right)\gamma^j q\left(\frac{z^-}{2}\right)|P,S\rangle = \frac{1}{2p^+}\bar{u}(P',S')\left[\frac{\Delta_\perp^j}{2M}G_1+\gamma^j(H+E+G_2)+\frac{\Delta_\perp^j}{p^+}\gamma^+G_3+\frac{i\epsilon_T^{jk}\Delta_\perp^k}{p^+}\gamma^+\gamma_5G_4\right]u(P,S), \tag{2}$$

$$\frac{1}{2}\int\frac{dz^-}{2\pi}e^{ixp^+z^-}\langle P',S'|\bar{q}\left(-\frac{z^-}{2}\right)\gamma^j\gamma_5 q\left(\frac{z^-}{2}\right)|P,S\rangle = \frac{1}{2p^+}\bar{u}(P',S')\left[\frac{\Delta_\perp^j}{2M}\gamma_5(\tilde{E}+\tilde{G}_1)+\gamma^j\gamma_5(\tilde{H}+\tilde{G}_2)+\frac{\Delta_\perp^j}{p^+}\gamma^+\gamma_5\tilde{G}_3+\frac{i\epsilon_T^{jk}\Delta_\perp^k}{p^+}\gamma^+\tilde{G}_4\right]u(P,S). \tag{3}$$

In Eqs. (2) and (3), $P(P')$ is the incoming (outgoing), p^+ is the average longitudinal nucleon four-momentum, $S(S')$ is the initial (final) nucleon spin, M is the nucleon mass, and $H, E, \tilde{H}, \tilde{E}$ are twist-2, $G_1, \ldots, G_4, \tilde{G}_1, \ldots, \tilde{G}_4$ are twist-3 GPDs.

In this study, we focus on the twist-3 GPDs G_2 and $\tilde{G}_2$ since they are essential in the sense that G_2 is related to the quark kinetic orbital angular momentum via Eq. (1), and $\tilde{G}_2$ reduces to $g_2(x)$ in the forward limit which enters the polarized deep inelastic scattering (DIS) cross section [36].

TABLE I. The behavior of the discontinuities of the twist-3 GPDs, $\tilde{G}_2$ and G_2, as $\xi \to 0$ in QTM and SDM.

Twist-3 GPD	QTM	SDM
G_2	Divergent	Divergent
$\tilde{G}_2$	Finite	Divergent

This paper is organized as follows: In Secs. II and III, the twist-3 GPDs G_2 and $\tilde{G}_2$ are calculated using QTM and SDM, respectively. The behaviors of their discontinuities under decreasing skewness parameters ($\xi \to 0$) are investigated and summarized in Table I. In Sec. IV, the forward limit of $\tilde{G}_2$, twist-3 PDF $g_2(x)$, is calculated using SDM. The discontinuities of $\tilde{G}_2$ are identified with a Dirac delta function term in $g_2(x)$. With the motivation of investigating the origin of this singularity, also the quasi-PDF, $g_2^{\mathrm{quasi}}(k^z)$, is calculated. Determining $g_2^{\mathrm{quasi}}(k^z)$ shows that the Dirac delta function term in $g_2(x)$ corresponds to a momentum component in the nucleon state that does not scale as the nucleon is boosted to the IMF. As shown in Sec. V, neglecting the Dirac delta functions leads to the violation of sum rules for twist-3 PDFs and GPDs. In Sec. VI, our work is summarized.

II. G_2 AND $\tilde{G}_2$ IN QUARK TARGET MODEL

In QTM, a quark or an antiquark releases a photon/gluon and recombines with it after the interaction. Figure 1 shows QTM in a symmetric frame where the kinematic variables are Δ, the four-momentum transfer; $P = p - \frac{\Delta}{2}$ $(P' = p + \frac{\Delta}{2})$, the incoming (outgoing) four-momentum; p, the average momentum (with $p_\perp = 0$); $k - \frac{\Delta}{2}$ $(k + \frac{\Delta}{2})$, the four-momentum before (after) the interaction.

To calculate G_2, the matrix element on the left-hand side (LHS) of Eq. (2) is written using QTM with the vertex operator, $\Gamma = \gamma^\perp$,

$$-\frac{ig^2}{2}\int\frac{d^4k}{(2\pi)^4}\delta(k^+-xp^+)\bar{u}(P',S')\gamma^\mu\frac{(\not{k}+\frac{\not{\Delta}}{2}+m)}{[(k+\frac{\Delta}{2})^2-m^2+i\epsilon]}\gamma^\perp\frac{(\not{k}-\frac{\not{\Delta}}{2}+m)}{[(k-\frac{\Delta}{2})^2-m^2+i\epsilon]}\gamma^\nu \times\left[g_{\mu\nu}-\frac{n_\nu(p_\mu-k_\mu)}{p^+-k^+}-\frac{n_\mu(p_\nu-k_\nu)}{p^+-k^+}\right]\frac{1}{[(p-k)^2-\lambda^2+i\epsilon]}u(P,S) = \frac{1}{2p^+}\bar{u}(P',S')\left[\frac{\Delta^\perp}{2M}G_1+\gamma^\perp(H+E+G_2)+\frac{\Delta^\perp}{p^+}\gamma^+G_3+\frac{i\epsilon_T^{\perp k}\Delta_k^\perp}{p^+}\gamma^+\gamma_5G_4\right]u(P,S), \tag{4}$$

and the coefficient of the vector structure, $(H + E + G_2)$, is identified. In Eq. (4), g is the coupling strength, $m = M$ is the quark/antiquark, and λ is the renormalization mass. To extract G_2 from the combination, $(H + E + G_2)$, H is calculated in QTM using the parametrization,

$$\frac{1}{2}\int\frac{dz^-}{2\pi}e^{ixp^+z^-}\langle P',S'|\bar{q}\left(-\frac{z^-}{2}\right)\gamma^+q\left(\frac{z^-}{2}\right)|P,S\rangle=\frac{1}{2p^+}\bar{u}(P',S')\left[\gamma^+H+\frac{i\sigma^{+\rho}\Delta_\rho}{2M}E\right]u(P,S). \tag{5}$$

For simplicity, only the divergent contributions are considered. Since E is finite, it does not contribute to the divergent parts of the matrix elements in Eqs. (4) and (5).

Identifying ξ with the longitudinal momentum transfer fraction ($\xi=\Delta^+/2p^+$), the three regions regarding the interval of the longitudinal momentum fraction ($x=k^+/p^+$) have to be distinguished to evaluate the k^- integrals on the LHS of Eq. (4):

(i) For $\xi<x\le 1$, the incoming and outgoing longitudinal momentum fractions, $x-\xi$ and $x+\xi$, are positive, and the correlator involves an incoming and an outgoing quark.

(ii) For $-\xi\le x\le\xi$, the incoming longitudinal momentum fraction, $x-\xi$, is negative and the outgoing, $x+\xi$, is positive. In this region, the correlator involves an incoming antiquark and outgoing quark.

(iii) For $-1\le x<\xi$, both momentum fractions are negative, describing an incoming and an outgoing antiquark.

The regions $\xi<x\le 1$ and $-1\le x<\xi$ are commonly referred to as Dokshitzer-Gribov-Lipatov-Altarelli-Parisi regions [37–40] and $-\xi\le x<\xi$ as the Efremov-Radyuskin-Brodsky-Lepage (ERBL) region [41,42]. Regarding these regions, the divergent part of G_2 in QTM is calculated as

$$G_2=\begin{cases}\frac{g^2}{\pi^2}\frac{(1+x)}{(1-\xi^2)}\ln\Lambda_\perp & \text{for } \xi<x<1,\\ -\frac{g^2}{2\pi^2}\frac{(1+x)}{\xi(1+\xi)}\ln\Lambda_\perp & \text{for } -\xi\le x\le\xi,\\ 0 & \text{for } -1<x<\xi,\end{cases} \tag{6}$$

where $\Lambda_\perp$ is the transverse momentum cutoff. Since it violates the conservation of momentum in QTM, the distribution does not have support in the $-1<x<\xi$ region.

To calculate $\tilde{G}_2$, the matrix element on the LHS of Eq. (3) is written using QTM with the vertex operator, $\Gamma=\gamma^\perp\gamma_5$, and the coefficient of the axial vector structure, $(\tilde{H}+\tilde{G}_2)$, is identified,

$$\begin{aligned}-\frac{ig^2}{2}\int\frac{d^4k}{(2\pi)^4}&\delta(k^+-xp^+)\bar{u}(P',S')\gamma^\mu\frac{(\not{k}+\frac{\not{\Delta}}{2}+m)}{[(k+\frac{\Delta}{2})^2-m^2+i\epsilon]}\gamma^\perp\gamma_5\frac{(\not{k}-\frac{\not{\Delta}}{2}+m)}{[(k-\frac{\Delta}{2})^2-m^2+i\epsilon]}\gamma^\nu\\ &\times\left[g_{\mu\nu}-\frac{n_\nu(p_\mu-k_\mu)}{p^+-k^+}-\frac{n_\mu(p_\nu-k_\nu)}{p^+-k^+}\right]\frac{1}{[(p-k)^2-\lambda^2+i\epsilon]}u(P,S)\\ =&\frac{1}{2p^+}\bar{u}(P',S')\left[\frac{\Delta^\perp}{2M}\gamma_5(\tilde{E}+\tilde{G}_1)+\gamma^\perp\gamma_5(\tilde{H}+\tilde{G}_2)+\frac{\Delta^\perp}{p^+}\gamma^+\gamma_5\tilde{G}_3+\frac{i\epsilon_T^{\perp k}\Delta_k^\perp}{p^+}\gamma^+\tilde{G}_4\right]u(P,S).\end{aligned} \tag{7}$$

$\tilde{H}$ is calculated in the same model, but with the vertex operator, $\Gamma=\gamma^+\gamma_5$, using the parametrization

$$\frac{1}{2}\int\frac{dz^-}{2\pi}e^{ixp^+z^-}\langle P',S'|\bar{q}\left(-\frac{z^-}{2}\right)\gamma^+\gamma_5q\left(\frac{z^-}{2}\right)|P,S\rangle=\frac{1}{2p^+}\bar{u}(P',S')\left[\gamma^+\gamma_5\tilde{H}+\frac{\gamma_5\Delta^+}{2M}\tilde{E}\right]u(P,S). \tag{8}$$

Considering only the divergent parts, where $\tilde{E}$ does not contribute to the matrix elements in Eqs. (7) and (8), $\tilde{G}_2$ is calculated as

$$\tilde{G}_2=\begin{cases}\frac{g^2}{\pi^2}\frac{(x+\xi^2)}{(1-\xi^2)}\ln\Lambda_\perp & \text{for } \xi<x<1,\\ -\frac{g^2}{2\pi^2}\frac{(x+\xi^2)}{\xi(1+\xi)}\ln\Lambda_\perp & \text{for } -\xi\le x\le\xi,\\ 0 & \text{for } -1<x<\xi.\end{cases} \tag{9}$$

As Fig. 2 shows, G_2 and $\tilde{G}_2$ exhibit discontinuities at the points $x=\pm\xi$ which correspond to vanishing longitudinal

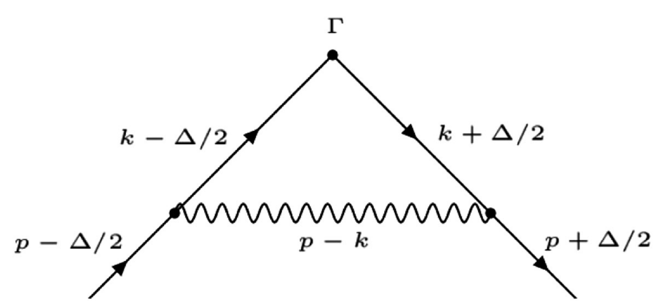

FIG. 1. QTM in a symmetric frame.

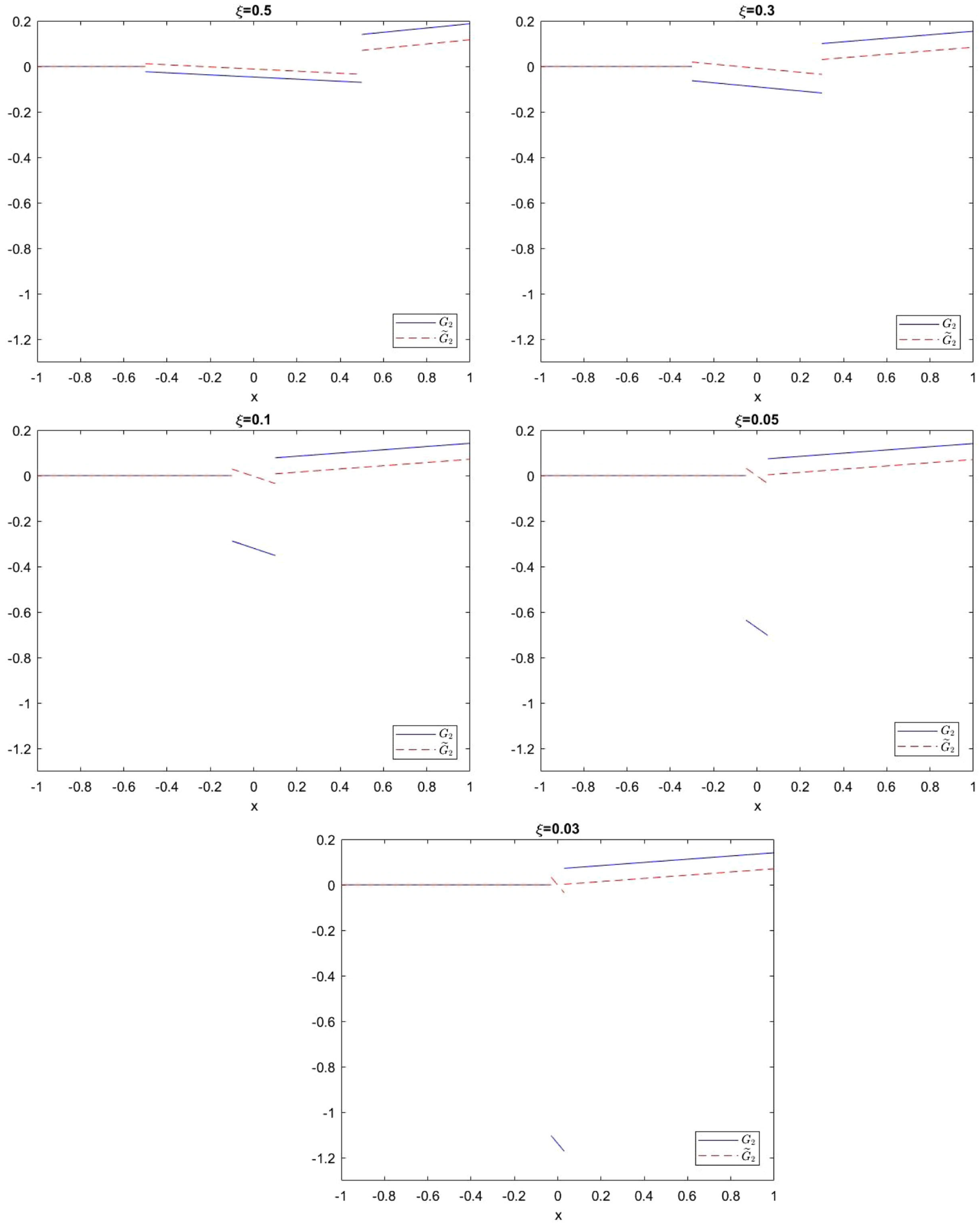

FIG. 2. Discontinuities of the twist-3 GPDs, G_2 and $\tilde{G}_2$ in QTM for $\Lambda_\perp = 2$, and $g = 1$.

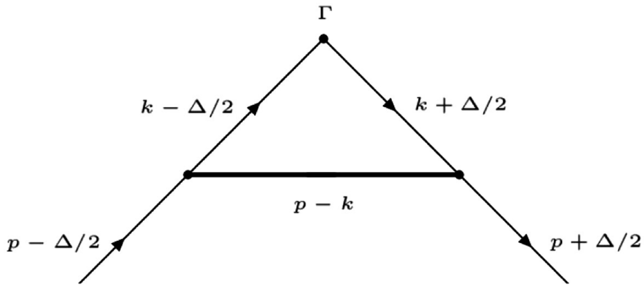

FIG. 3. SDM in a symmetric frame.

momentum components in the initial or final state. In the limit of $\xi \to 0$, the discontinuities of $\tilde{G}_2$ stay finite, and the contribution from the ERBL region partially cancels upon integrating over x. Whereas, the discontinuities of G_2 diverge, and its ERBL region resembles a representation of a Dirac delta function, as explained in Appendix A. In the following section, the discontinuities of G_2 and $\tilde{G}_2$ and their behaviors as $\xi \to 0$ are investigated using SDM.

III. G_2 AND $\tilde{G}_2$ IN SCALAR DIQUARK MODEL

In a SDM, the three valence quarks of the nucleon are considered to be a bound state of a single quark and a scalar diquark. We assume that the virtual photon is interacting only with the single quark (active quark) and the scalar diquark is a spectator as shown in Fig. 3.

To calculate G_2, the matrix element on the LHS of Eq. (2) is written using SDM,

$$\frac{ig^2}{2}\int\frac{d^4k}{(2\pi)^4}\delta(k^+-xp^+)\bar{u}(P',S')\frac{(\not{k}+\frac{\not{\Delta}}{2}+m)}{[(k+\frac{\Delta}{2})^2-m^2+i\epsilon]}\gamma^\perp\frac{(\not{k}-\frac{\not{\Delta}}{2}+m)}{[(k-\frac{\Delta}{2})^2-m^2+i\epsilon]}\frac{1}{[(p-k)^2-\lambda^2+i\epsilon]}u(P,S)$$
$$=\frac{1}{2p^+}\bar{u}(P',S')\left[\frac{\Delta^\perp}{2M}G_1+\gamma^\perp(H+E+G_2)+\frac{\Delta^\perp}{p^+}\gamma^+G_3+\frac{i\epsilon_T^{\perp k}\Delta_k^\perp}{p^+}\gamma^+\gamma_5G_4\right]u(P,S), \tag{10}$$

and the coefficient of the vector structure, $(H+E+G_2)$, is identified. In Eq. (10), M, m, and λ denote the nucleon, quark, and diquark masses, respectively. G_2 is extracted considering only the divergent contributions, as in the QTM case,

$$G_2=\begin{cases}-\frac{g^2}{2\pi^2}\frac{(1-x)}{(1-\xi^2)}\ln\Lambda_\perp & \text{for } \xi<x<1,\\ -\frac{g^2}{8\pi^2}\frac{(2x+\xi-1)}{\xi(1+\xi)}\ln\Lambda_\perp & \text{for } -\xi\le x\le\xi,\\ 0 & \text{for } -1<x<\xi.\end{cases} \tag{11}$$

To calculate $\tilde{G}_2$, the matrix element in Eq. (3) is written using SDM,

$$\frac{ig^2}{2}\int\frac{d^4k}{(2\pi)^4}\delta(k^+-xp^+)\bar{u}(P',S')\frac{(\not{k}+\frac{\not{\Delta}}{2}+m)}{[(k+\frac{\Delta}{2})^2-m^2+i\epsilon]}\gamma^\perp\gamma_5\frac{(\not{k}-\frac{\not{\Delta}}{2}+m)}{[(k-\frac{\Delta}{2})^2-m^2+i\epsilon]}\frac{1}{[(p-k)^2-\lambda^2+i\epsilon]}u(P,S)$$
$$=\frac{1}{2p^+}\bar{u}(P',S')\left[\frac{\Delta^\perp}{2M}\gamma_5(\tilde{E}+\tilde{G}_1)+\gamma^\perp\gamma_5(\tilde{H}+\tilde{G}_2)+\frac{\Delta^\perp}{p^+}\gamma^+\gamma_5\tilde{G}_3+\frac{i\epsilon_T^{\perp k}\Delta_k^\perp}{p^+}\gamma^+\tilde{G}_4\right]u(P,S), \tag{12}$$

the axial vector structure coefficient, $(\tilde{H}+\tilde{G}_2)$, is identified, and after calculating $\tilde{H}$, the divergent part of $\tilde{G}_2$ is obtained,

$$\tilde{G}_2=\begin{cases}-\frac{g^2}{2\pi^2}\frac{(x-\xi^2)}{(1-\xi^2)}\ln\Lambda_\perp & \text{for } \xi<x<1,\\ \frac{g^2}{8\pi^2}\frac{(2x-2\xi^2+\xi+1)}{\xi(1+\xi)}\ln\Lambda_\perp & \text{for } -\xi\le x\le\xi,\\ 0 & \text{for } -1<x<\xi.\end{cases} \tag{13}$$

As shown in Fig. 4, G_2 and $\tilde{G}_2$ exhibit discontinuities at the points $x=\pm\xi$. These discontinuities diverge as $\xi\to 0$, and the ERBL regions of both GPDs resemble a representation of a Dirac delta function.

The behaviors of the discontinuities of $\tilde{G}_2$ and G_2 as $\xi\to 0$ in QTM and SDM are summarized in Table I. In the following section, twist-3 PDFs and quasi-PDFs are investigated using SDM.

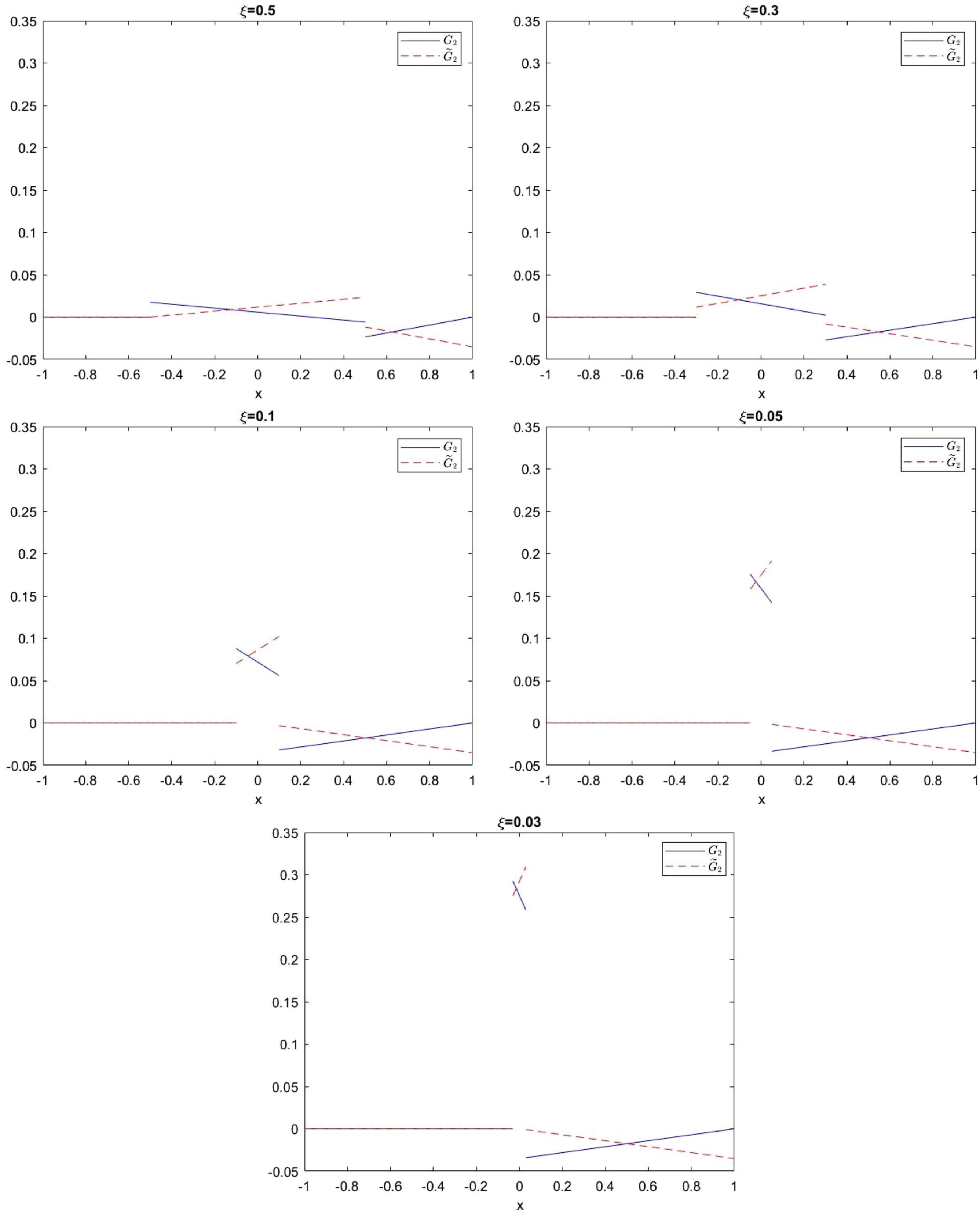

FIG. 4. Discontinuities of the twist-3 GPDs, G_2 and $\tilde{G}_2$, in SDM for $\Lambda_\perp = 2$ and $g = 1$.

IV. TWIST-3 PDFS AND TWIST-3 QUASI-PDFS IN SCALAR DIQUARK MODEL

For equal momenta and spins of the initial and final hadron states, the matrix elements defining GPDs reduce to the matrix elements defining PDFs [43]. There are three quark PDFs (f_1, g_1, h_1) at twist-2 level and three quark PDFs (e, h_L, g_2) at twist-3 level. The complete set of PDFs is defined by the matrix elements of quark bilocal operators,

$$\int \frac{d\lambda}{2\pi} e^{i\lambda x} \langle P,S|\bar{q}(0)\gamma^\mu q(\lambda n)|P,S\rangle = 2[f_1(x)\hat{p}^\mu + M^2 f_4(x)\hat{n}^\mu], \tag{14}$$

$$\int \frac{d\lambda}{2\pi} e^{i\lambda x} \langle P,S|\bar{q}(0)\gamma^\mu\gamma_5 q(\lambda n)|P,S\rangle = 2\{g_1(x)\hat{p}^\mu(S\cdot\hat{n}) + g_T(x)S_\perp^\mu + M^2 g_3(x)\hat{n}^\mu(S\cdot\hat{n})\}, \tag{15}$$

$$\int \frac{d\lambda}{2\pi} e^{i\lambda x} \langle P,S|\bar{q}(0)q(\lambda n)|P,S\rangle = 2Me(x), \tag{16}$$

$$\int \frac{d\lambda}{2\pi} e^{i\lambda x} \langle P,S|\bar{q}(0)i\sigma^{\mu\nu}\gamma_5 q(\lambda n)|P,S\rangle = 2\left[h_1(x)\frac{(S_\perp^\mu \hat{p}^\nu - S_\perp^\nu \hat{p}^\mu)}{M} + h_L(x)M(\hat{p}^\mu\hat{n}^\nu - \hat{p}^\nu\hat{n}^\mu)S\cdot\hat{n} + h_3(x)M(S_\perp^\mu\hat{n}^\nu - S_\perp^\nu\hat{n}^\mu)\right], \tag{17}$$

where P, S, and M are the momentum, spin, and mass of the parent hadron, respectively. $\hat{p}$ and $\hat{n}$ are lightlike vectors, i.e., $\hat{p}^2 = \hat{n}^2 = 0$, with the components, $\hat{p}^- = \hat{p}_\perp = 0$, $\hat{p}^+ = P^+$ and $\hat{n}^+ = \hat{n}_\perp = 0, \hat{n}^- = 1/P^+$. The spin vector, S^μ, is decomposed as $S^\mu = (S\cdot\hat{n})\hat{p}^\mu + (S\cdot\hat{p})\hat{n}^\mu + S_\perp^\mu$. x represents the parton's light-cone momentum fraction and each PDF has a support in the $-1 \leq x \leq 1$ interval. The PDFs, f_4, g_3, and h_3 appear at twist-4 level. In the parametrization given by Eq. (15), $g_T(x) = g_1(x) + g_2(x)$.

Even though the matrix elements entering the cross section are usually dominated by twist-2 operators in the Bjorken limit, and twist-3 operators are mostly relevant for subleading corrections, the twist-3 PDFs, $g_2(x)$ and $h_L(x)$, are unique in the sense that they appear as leading contributions in some spin asymmetries. For example, $g_2(x)$ can be measured in the transversely polarized DIS, and $h_L(x)$ can be measured in the longitudinal-transverse double spin asymmetry in the polarized Drell-Yan process [44].

The twist-3 GPD, $\tilde{G}_2$, reduces to the twist-3 PDF, $g_2(x)$, in the forward limit. In order to investigate the Dirac delta function behavior of $\tilde{G}_2$ in the ERBL region in the forward limit, $g_2(x) = g_T(x) - g_1(x)$ is calculated using Fig. 5, as explained in Appendix A.

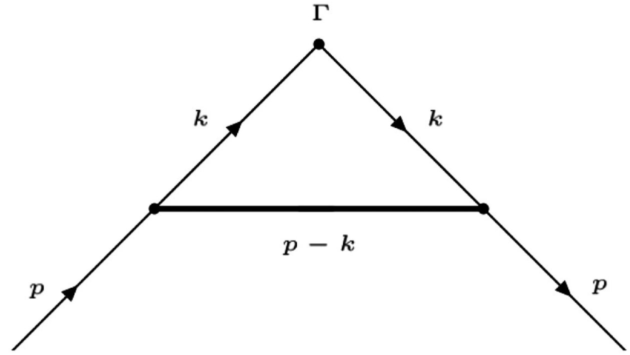

FIG. 5. SDM in the forward limit.

$g_2(x)$ contains the following term which contains a singularity:

$$g_{2,\delta}(k^+) = -\frac{ig^2}{(2\pi)^2}\frac{(k^+ + \frac{m}{M}P^+)}{(P^+ - k^+)}\int \frac{d^2k_\perp}{(2\pi)^2}\frac{dk^-}{(k^2 - m^2 + i\epsilon)^2}, \tag{18}$$

where m is the quark and M is the nucleon mass.

The singularity originates from the light-cone energy integral,

$$\int \frac{dk^-}{(k^2 - m^2 + i\epsilon)^2}, \tag{19}$$

which is performed using Cauchy's theorem. Obviously, for $k^+ \neq 0$,

$$\int \frac{dk^-}{(k^2 - m^2 + i\epsilon)^2} = \int \frac{dk^-}{[2k^+(k^- - \frac{(k_\perp^2 + m^2)}{2k^+} + \frac{i\epsilon}{2k^+})]^2} = 0, \tag{20}$$

since enclosing the double pole, $k^- = \frac{(k_\perp^2 + m^2)}{2k^+} - \frac{i\epsilon}{2k^+}$, can be avoided by closing the contour in the appropriate half-plane of the complex k^- plane. However, when $k^+ = 0$ is included, the result of this integral is not zero,

$$\int dk^+ dk^- \frac{1}{(k^2 - m^2 + i\epsilon)^2} = \int dk^+ dk^- \frac{1}{(2k^+k^- - k_\perp^2 - m^2 + i\epsilon)^2} = \frac{i\pi}{k_\perp^2 + m^2}. \tag{21}$$

Thus, combining Eq. (20) with Eq. (21) implies that[1]

[1]This result has been first derived in Ref. [45].

$$\int \frac{dk^-}{(k^2 - m^2 + i\epsilon)^2} = \frac{i\pi}{k_\perp^2 + m^2}\delta(k^+). \tag{22}$$

Therefore, the singular term is

$$g_{2,\delta}(k^+) = -\frac{ig^2}{(2\pi)^2}\frac{(k^+ + \frac{m}{M}P^+)}{(P^+ - k^+)}\int \frac{d^2k_\perp}{(2\pi)^2}\frac{dk^-}{(k^2 - m^2 + i\epsilon)^2}$$
$$= \frac{g^2}{16\pi^2}\frac{(k^+ + \frac{m}{M}P^+)}{(P^+ - k^+)}\ln\left(\frac{\Lambda_\perp^2 + m^2}{m^2}\right)\delta(k^+), \tag{23}$$

where $\Lambda_\perp$ is the transverse momentum cutoff.

The term in Eq. (23) is given in terms of longitudinal momentum, k^+. In order to express it as a function of the longitudinal momentum fraction, it is integrated over k^+ and multiplied by P^+,

$$g_{2,\delta}(x) = \frac{g^2}{16\pi^2}\frac{(x + \frac{m}{M})}{(1 - x)}\ln\left(\frac{\Lambda_\perp^2 + m^2}{m^2}\right)\delta(x). \tag{24}$$

To illustrate the origin of the Dirac delta function contribution, now we consider the twist-3 quasi-PDF, $g_2^{\rm quasi}(x)$. While PDFs are calculated using light-cone coordinates, when calculating quasi-PDFs one treats the operators in normal coordinates where the nucleon moves purely in a spatial direction with a momentum P^z [46,47]. PDFs are recovered from quasi-PDFs by taking the $P^z \to \infty$ limit [48–50].

In addition, we also consider the distributions as functions of longitudinal momenta, i.e., $g_2(k^+)$ and $g_2^{\rm quasi}(k^z)$, as shown in Fig. 6.[2] The twist-3 distributions are identified by their scaling property under a longitudinal nucleon momentum boost: Twist-3 PDFs scale with $1/P^+$, and twist-3 quasi-PDFs with $1/P^z$. Whereas the distributions in Fig. 6 have two components, one of which obeys the twist-3 scaling properties, while the other component at $k^z(k^+) = 0$ does not scale as the nucleon is boosted to higher longitudinal momenta. In other words, the $k^z(k^+) = 0$ component does not change with $1/P^z(1/P^+)$.

The nonscaling component of the PDF $g_2(k^+)$ corresponds to the term $g_{2,\delta}(k^+)$ given by Eq. (23), while the nonscaling (ns) component of the quasi-PDF $g_2^{\rm quasi}(k^z)$ originates from the term,

$$g_{2,\rm ns}^{\rm quasi}(k^z) = -\frac{g^2}{16\pi^2}\frac{m}{M}\frac{1}{(k_\perp^2 + k_z^2 + m^2)^{1/2}}\Bigg|_{k_\perp=0}^{\Lambda_\perp}. \tag{25}$$

Figure 7 shows the distributions as functions of x where the expression in Eq. (25) is multiplied by P^z. It can be seen that the nonscaling component of the quasi-PDF $g_2^{\rm quasi}(x)$ can be identified with a representation of a Dirac delta function at $x = 0$ as the nucleon is boosted to the IMF, i.e., $P^z \to \infty$.

Operator product expansion (OPE) analysis of the matrix elements allows the twist-3 distributions to be decomposed into the contributions expressed in terms of twist-2 distributions (WW part) [31], a quark mass term, and the rest which involve interactions. For example, for $g_2(x)$ the decomposition reads

$$g_2(x) = g_2^{\rm WW}(x) + g_2^m(x) + \bar{g}_2(x), \tag{26}$$

where the WW part is given by [51]

$$g_2^{\rm WW}(x) = -g_1(x) + \int_x^1 \frac{dy}{y}g_1(y). \tag{27}$$

In QCD, $\bar{g}_2(x)$ corresponds to the pure quark-gluon correlation part of the twist-3 distribution. These pure quark-gluon correlations, which are also called *genuine twist-3* terms, involve a novel type of information that is not contained in twist-2 distributions. For example, the x^2 moment of the genuine twist-3 part of polarized PDF $\bar{g}_2(x)$ can be identified with the transverse component of the average color Lorentz force acting on the struck quark at the instant after absorbing the virtual photon [12].

An important question is, whether the components which do not scale under a longitudinal momentum boost come from the WW parts of twist-3 distributions. In order to address this question, in addition to $g_1(x)$ and $g_2(x)$, also the twist-2 PDFs $f_1(x)$, $h_1(x)$, and twist-3 pdfs $e(x)$, $h_L(x)$ are calculated using SDM. The PDFs calculated with QTM are taken from Ref. [52].

As shown in Table II, all the twist-3 PDFs calculated in SDM and QTM contain a $\delta(x)$ term only with the exception of $g_2(x)$ in QTM, whereas such a term does not appear in any of the twist-2 PDFs. As an example, the twist-2 PDF $g_1(x)$ and the twist-2 quasi-PDF $g_1^{\rm quasi}(x)$ are calculated in SDM. Figure 8 shows that $g_1^{\rm quasi}(x)$ converges to $g_1(x)$ as $P^z \to \infty$ without generating a $\delta(x)$. Therefore, any potential singularity which can result from the integral in Eq. (27) does not originate from Eq. (19). For this reason, the WW part is not the source of the $\delta(x)$ contribution in a twist-3 distribution.

As another example, twist-3 PDF $e(k^+)$ and quasi-PDF $e^{\rm quasi}(k^z)$ are shown in Fig. 9. As the nucleon is boosted to the IMF, $e^{\rm quasi}(k^z)$ converges to $e(k^+)$. $e(k^+)$ contains a $\delta(k^+)$ term which corresponds to a nonscaling term in

[2]For simplicity, the masses M, m, and λ are set to "1" to obtain the plots of the PDFs and the quasi-PDFs. Therefore, the quantities, which carry the units of those masses, are dimensionless. Consequently, the transverse momentum cutoff, $\Lambda_\perp$, the longitudinal quark momenta, $k^z(k^+)$, and the longitudinal nucleon momenta, $P^z(P^+)$, in Figs. 6, 7, 8, 9, and 10 do not have units.

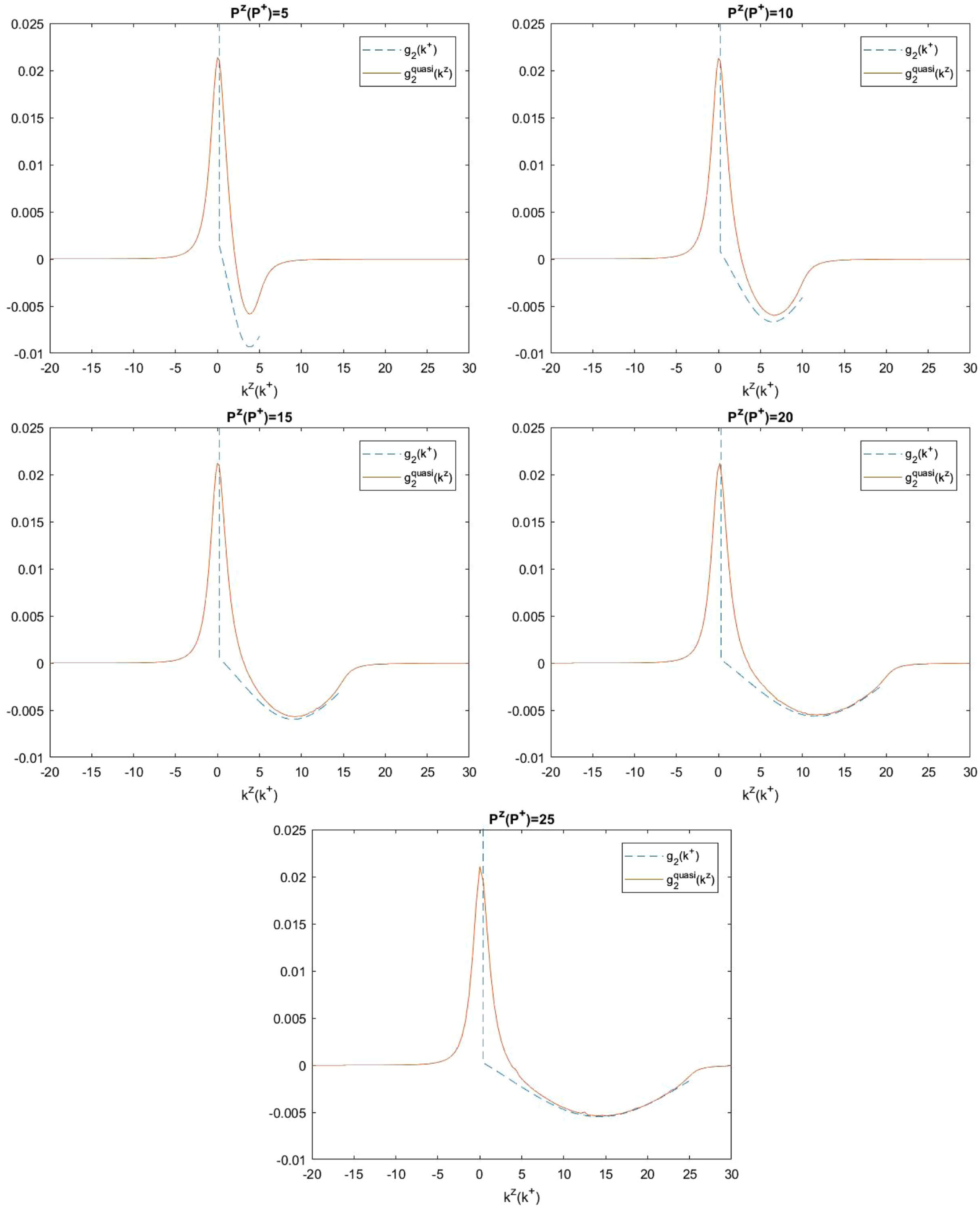

FIG. 6. $g_2(k^+)$ and $g_2^{\mathrm{quasi}}(k^z)$ in SDM for $m = M = \lambda = 1$ and $\Lambda_\perp = 2$.

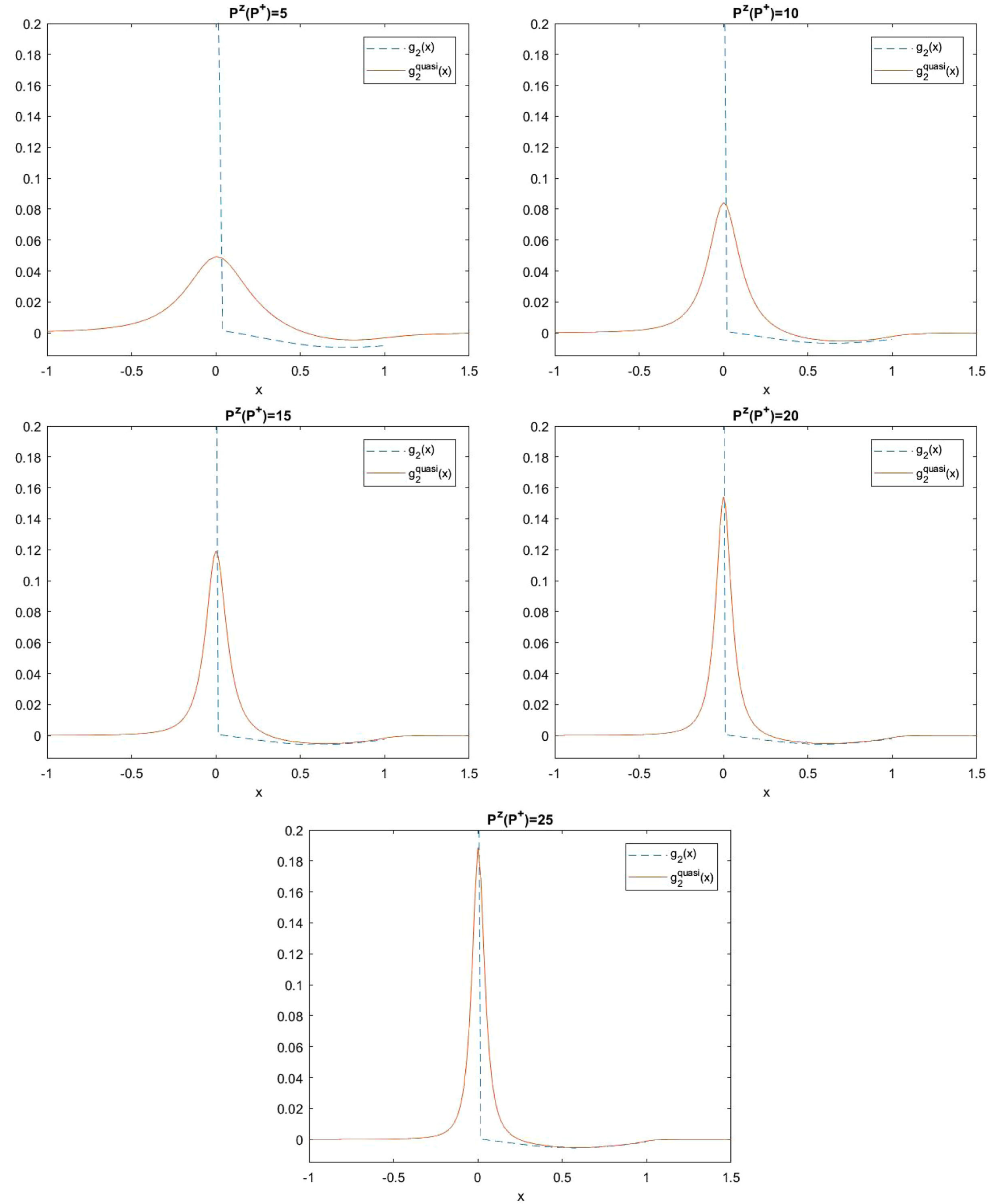

FIG. 7. $g_2(x)$ and $g_2^{\mathrm{quasi}}(x)$ in SDM for $m = M = \lambda = 1$ and $\Lambda_\perp = 2$. $x = \frac{k^+}{P^+}$ for $g_2(x)$ and $x = \frac{k^z}{P^z}$ for $g_2^{\mathrm{quasi}}(x)$.

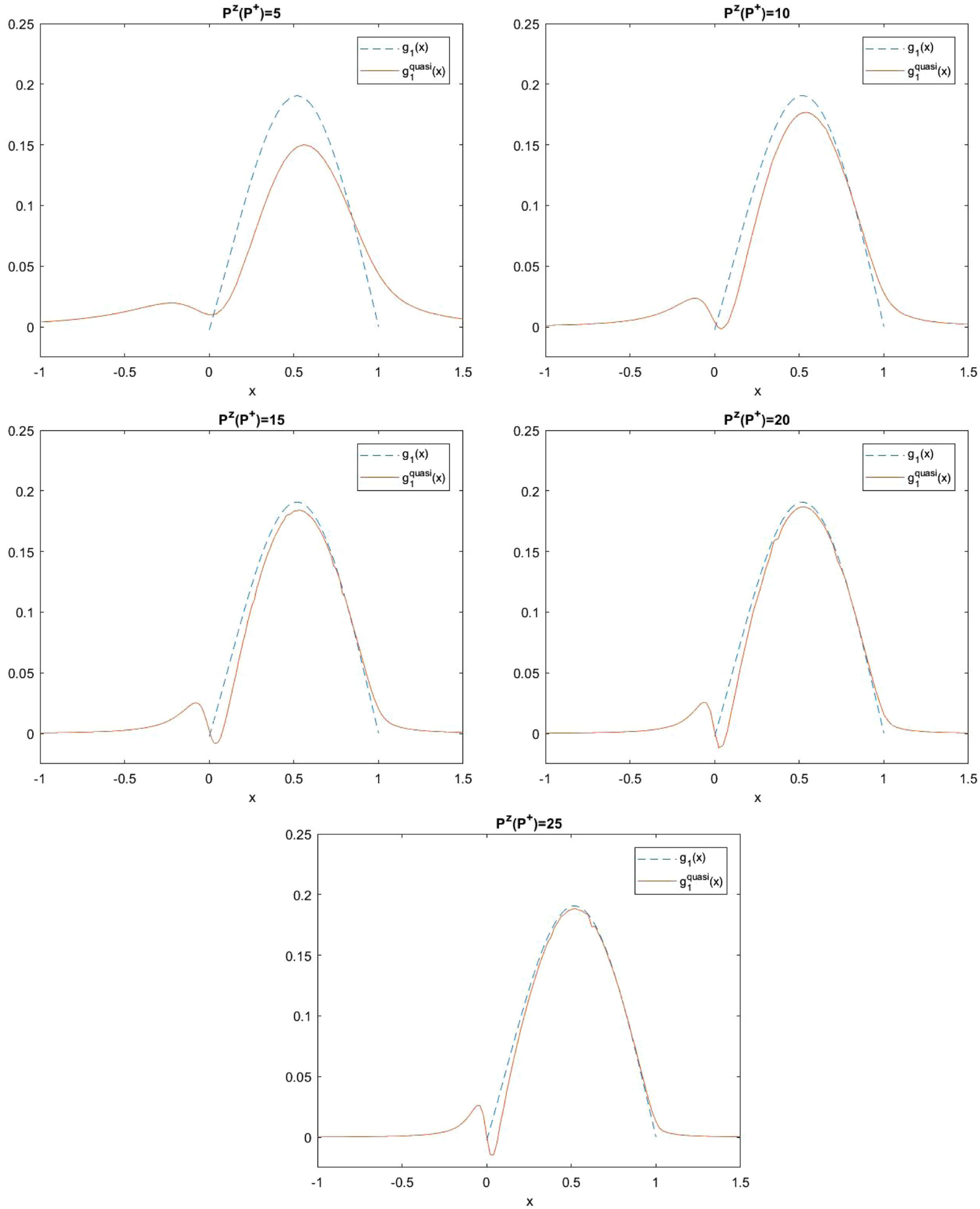

FIG. 8. $g_1(x)$ and $g_1^{\text{quasi}}(x)$ in SDM for $m = M = \lambda = 1$ and $\Lambda_\perp = 2$. $x = \frac{k^+}{P^+}$ for $g_1(x)$ and $x = \frac{k^z}{P^z}$ for $g_1^{\text{quasi}}(x)$.

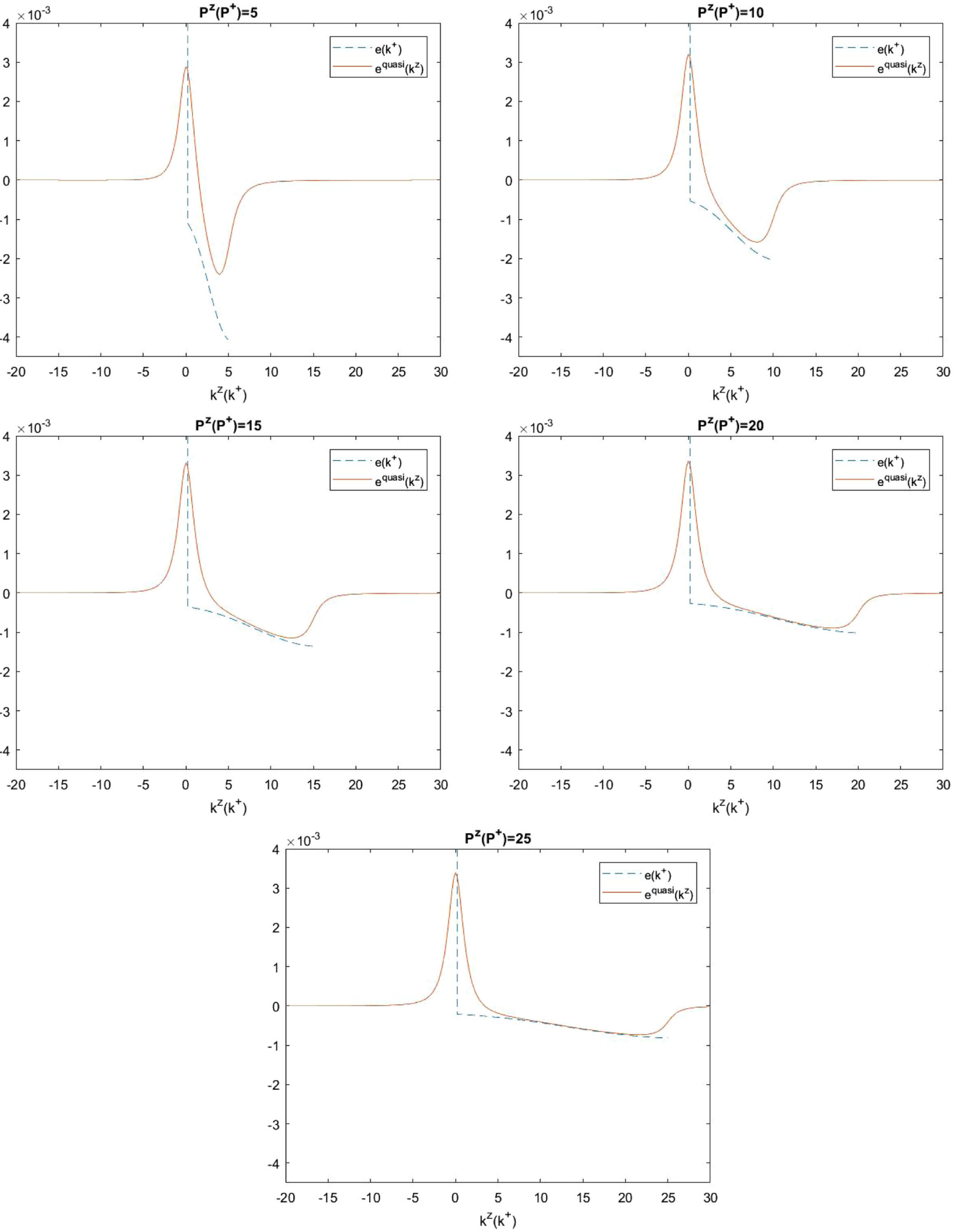

FIG. 9. $e(k^+)$ and $e^{\mathrm{quasi}}(k^z)$ in SDM for $m = M = \lambda = 1$ and $\Lambda_\perp = 2$.

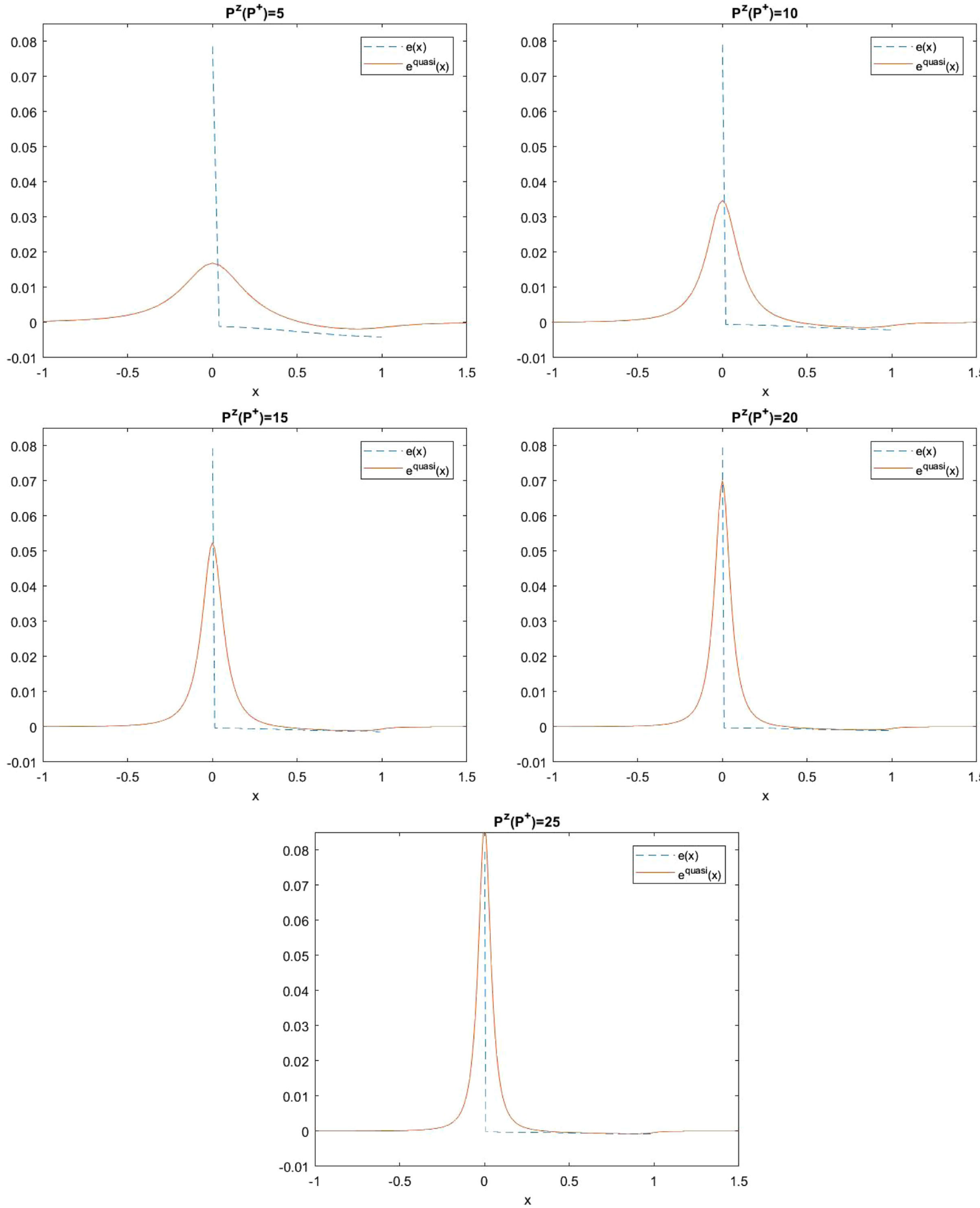

FIG. 10. $e(x)$ and $e^{\mathrm{quasi}}(x)$ in SDM for $m = M = \lambda = 1$ and $\Lambda_\perp = 2$. $x = \frac{k^+}{P^+}$ for $e(x)$ and $x = \frac{k^z}{P^z}$ for $e^{\mathrm{quasi}}(x)$.

TABLE II. Dirac delta functions in PDFs calculated using SDM and QTM. ✗ denotes there is no $\delta(x)$ and ✓ denotes there is a $\delta(x)$ in a PDF.

Twist-2 PDF	SDM	QTM
$f_1(x)$	✗	✗
$g_1(x)$	✗	✗
$h_1(x)$	✗	✗
Twist-3 PDF	SDM	QTM
$e(x)$	✓	✓
$h_L(x)$	✓	✓
$g_2(x)$	✓	✗

$e^{\text{quasi}}(k^z)$ at $k^z = 0$ as $P^z \to \infty$. Figure 10 shows that this component becomes a representation of $\delta(x)$ in $e^{\text{quasi}}(x)$ as the nucleon is boosted to the IMF.

There are several studies in which the singularity of $e(x)$ was discussed using the chiral quark soliton model [53–56]. The main difference is, in pQCD calculations, such as scalar diquark and quark target models, the delta functions arise from rainbow type diagrams while in the chiral quark soliton model, they arise from quark loops.

V. VIOLATION OF SUM RULES

The following sum rules for twist-3 distributions involve the point $x = 0$,

$$\int_{-1}^{1} dx g_1(x) = \int_{-1}^{1} dx g_T(x), \tag{28}$$

$$\int_{-1}^{1} dx h_1(x) = \int_{-1}^{1} dx h_L(x), \tag{29}$$

$$\int_{-1}^{1} dx e(x) = \frac{1}{2M}\langle P|\bar{\psi}(0)\psi(0)|P\rangle = \frac{d}{dm}M. \tag{30}$$

However, this point cannot be achieved in DIS experiments since x is defined as $x = \frac{Q^2}{2P\cdot q}$ and $x = 0$ corresponds to $P \cdot q \to \infty$. Therefore, experimental measurements cannot confirm but would rather claim the violation of these sum rules even though they are direct consequences of Lorentz invariance.

For example, Lorentz invariance of twist-3 GPDs imply that

$$\int_{-1}^{1} dx G_i(x,\xi,\Delta) = 0, \qquad \int_{-1}^{1} dx \tilde{G}_i(x,\xi,\Delta) = 0. \tag{31}$$

If $x = 0$ and hence the $\delta(x)$ are not included, Eq. (31) is violated as follows:

$$\lim_{\epsilon\to 0}\int_{-1}^{\epsilon} dx G_i(x,\xi=0,\Delta) + \lim_{\epsilon\to 0}\int_{\epsilon}^{1} dx G_i(x,\xi=0,\Delta) \neq 0, \tag{32}$$

$$\lim_{\epsilon\to 0}\int_{-1}^{\epsilon} dx \tilde{G}_i(x,\xi=0,\Delta) + \lim_{\epsilon\to 0}\int_{\epsilon}^{1} dx \tilde{G}_i(x,\xi=0,\Delta) \neq 0. \tag{33}$$

The Lorentz invariance relations in Eq. (31) can be regarded as a nonforward generalization of the Burkhardt-Cottingham sum rule given in Eq. (28) [57]. Since the LHS of Eq. (28) is the axial charge, the integral on the right-hand side (RHS) is finite. If the twist-3 PDF, $g_T(x)$, has a contribution proportional to $\delta(x)$ and $g_1(x)$ does not, experimental measurements would not be able to confirm this sum rule. Similar arguments apply to the h and σ-term sum rules in Eqs. (29) and (30), respectively. Therefore, the violation of the sum rules from the experimental data would provide indirect evidence on the existence of the Dirac delta functions.

VI. SUMMARY AND DISCUSSION

We have investigated the twist-3 GPDs G_2 and $\tilde{G}_2$ using QTM and SDM. In both models, these twist-3 GPDs exhibit discontinuities at the points $x = \pm\xi$. In the limit $\xi \to 0$, the discontinuities of G_2 are divergent in both models, and the ERBL region resembles a representation of a $\delta(x)$. However, the discontinuities of $\tilde{G}_2$ behave differently in the two different models: they diverge in SDM but stay finite in the QTM as $\xi \to 0$.

In the forward limit, $\tilde{G}_2$ reduces to $g_2(x)$, and the discontinuities grow into a $\delta(x)$ in SDM. Calculation of the quasi-PDF $g_2^{\text{quasi}}(k^z)$ reveals that the $\delta(x)$ term corresponds to a component that does not scale as the nucleon is boosted to the IMF.

The $\delta(x)$ contribution is not unique to the case of $g_2(x)$, and all the other twist-3 PDFs contain a $\delta(x)$ in both QTM and SDM only with the exception of $g_2(x)$ in the QTM. These $\delta(x)$ terms are not related to the twist-2 (WW) parts of the twist-3 PDFs since model calculations show that none of the twist-2 PDFs contain such a term. Violations of the sum rules containing twist-3 PDFs and GPDs experimentally would provide indirect evidence on the existence of these $\delta(x)$ contributions.

In effective field theories with four fermion interaction vertices, singularities in GPDs and PDFs may already arise at the twist-2 level [58]. However, the singularities we have discussed that arise for QCD and Yukawa type interactions are restricted to twist-3 or higher.

In generalized tadpole diagrams, i.e., diagrams where a subdiagram is connected to the rest of the diagram at a single vertex, the appearance of $\delta(x)$ terms is trivial: there is no momentum flowing through the subdiagram, and its contribution to the PDF does not scale in the IMF. However, the appearance of $\delta(x)$ is not trivial for the rainbowlike diagrams considered here, and we demonstrated that for higher twist PDFs there still appears such a component.

An important remark is, how the Delta function is effected by QCD evolution, i.e., its Q^2 dependence which can be related to the transverse momentum cutoff, $\Lambda_\perp$. In the model calculation, performed in Sec. IV, the $\delta(x)$ appears as the nucleon is boosted to the IMF regardless of the value of $\Lambda_\perp$, even though its coefficient evolves with $\Lambda_\perp^2$. Therefore, QCD evolution affects the coefficient of the $\delta(x)$ but its existence is a Q^2 independent result.

Integrals with similar pole structures to that of Eq. (19) such as

$$\int \frac{dk^-}{k^2 - m^2 + i\epsilon} \tag{34}$$

have been studied in connection with the light front vacuum [59–61]. The integrals involving the higher powers of the denominator in Eq. (34) can be obtained by repeated differentiation with respect to m^2. The relation between the light front vacuum and the $\delta(x)$ in twist-3 PDFs will be studied in Ref. [62].

ACKNOWLEDGMENTS

We thank C. Lorcé, A. Metz, and B. Pasquini for helpful discussions. This work was partially supported by the DOE under Grant No. DE-FG03-95ER40965.

APPENDIX A: G_2 IN QTM

The divergent part of G_2 is calculated as

$$-ig^2 \int \frac{d^2k_\perp dk^-}{(2\pi)^4} \frac{k^- 8(p^+)^2(1+x)}{[(k+\frac{\Delta}{2})^2 - m^2 + i\epsilon][(k-\frac{\Delta}{2})^2 - m^2 + i\epsilon][(p-k)^2 - \lambda^2 + i\epsilon]}. \tag{A1}$$

k^- in the numerator of Eq. (A1) can be replaced by the expression

$$k^- = \frac{m^2}{2p^+} - \frac{[(p-k)^2 - \lambda^2]}{2(p^+ - k^+)} - \frac{(k_\perp^2 + \lambda^2)}{2(p^+ - k^+)}. \tag{A2}$$

The second term in Eq. (A2) cancels the propagator in the denominator in Eq. (A1) leading to the following contribution which is nonzero only in the ERBL region, $-\xi < x < \xi$:

$$ig^2 4p^+ \frac{(1+x)}{(1-x)} \int \frac{d^2k_\perp dk^-}{(2\pi)^4} \frac{1}{[(k+\frac{\Delta}{2})^2 - m^2 + i\epsilon][(k-\frac{\Delta}{2})^2 - m^2 + i\epsilon]}. \tag{A3}$$

The result of this integral is dominated by the following term which diverges as $\xi \to 0$ yielding a representation of $\delta(x)$:

$$-\frac{g^2}{2\pi^2} \frac{(1+x)}{\xi(1-x)} \ln \Lambda_\perp. \tag{A4}$$

APPENDIX B: $\tilde{G}_2$ IN QTM

The divergent part of $\tilde{G}_2$ is calculated as

$$-ig^2 \int \frac{d^2k_\perp dk^-}{(2\pi)^4} \frac{k^- 8(p^+)^2(x+\xi^2)}{[(k+\frac{\Delta}{2})^2 - m^2 + i\epsilon][(k-\frac{\Delta}{2})^2 - m^2 + i\epsilon][(p-k)^2 - \lambda^2 + i\epsilon]}. \tag{B1}$$

Similarly, k^- in the numerator of Eq. (B1) can be replaced by the expression given by Eq. (A2) where the second term cancels the propagator in the denominator leading to the contribution,

$$ig^2 4p^+ \frac{(x+\xi^2)}{(1-x)} \int \frac{d^2k_\perp dk^-}{(2\pi)^4} \frac{1}{[(k+\frac{\Delta}{2})^2 - m^2 + i\epsilon][(k-\frac{\Delta}{2})^2 - m^2 + i\epsilon]}. \tag{B2}$$

The result of this integral is dominated by the term

$$-\frac{g^2}{2\pi^2}\frac{(x+\xi^2)}{\xi(1-x)}\ln\Lambda_\perp. \tag{B3}$$

Due to the appearance of ξ^2 in the numerator, this expression is finite as $\xi\to 0$, unlike the expression in Eq. (A4).

APPENDIX C: $g_T(x)$ IN SDM

$g_T(x)$ is obtained by using $\gamma^\mu=\gamma^\perp$ in the parametrization given by Eq. (15),

$$\int\frac{d\lambda}{2\pi}e^{i\lambda x}\langle P,S|\bar{q}(0)\gamma^\perp\gamma_5 q(\lambda n)|P,S\rangle = 2g_T(x)S^\perp. \tag{C1}$$

The LHS of Eq. (C1) is written using SDM,

$$g_T(x)S^\perp = \frac{ig^2}{2}\int\frac{d^4k}{(2\pi)^4}\delta(k^+-xP^+)\bar{u}(p)\times\frac{(\not{k}+m)}{(k^2-m^2+i\epsilon)}\gamma^\perp\gamma_5\frac{(\not{k}+m)}{(k^2-m^2+i\epsilon)}u(p)\times\frac{1}{[(p-k)^2-\lambda^2+i\epsilon]}. \tag{C2}$$

Using the identities,

$$\bar{u}(P)u(P)=2M, \tag{C3}$$

$$\bar{u}(P)\gamma^\mu u(P)=2P^\mu, \tag{C4}$$

$$\bar{u}(P)\gamma_5 u(P)=0, \tag{C5}$$

$$\bar{u}(P)\gamma^\mu\gamma_5 u(P)=2S^\mu, \tag{C6}$$

$$\bar{u}(P)\gamma^+\gamma^\perp\gamma_5 u(P)=\frac{2P^+}{M}S^\perp, \tag{C7}$$

$$\bar{u}(P)\gamma^-\gamma^\perp\gamma_5 u(P)=\frac{2P^-}{M}S^\perp=\frac{M}{P^+}S^\perp, \tag{C8}$$

$$\bar{u}(P)\gamma^-\gamma^+\gamma_5 u(P)=\frac{2M}{P^+}S^+, \tag{C9}$$

the numerator of the integrand in Eq. (C2) is calculated as

$$\bar{u}(P)(\not{k}+m)\gamma^\perp\gamma_5(\not{k}+m)u(P) = 2\left(x+\frac{m}{M}\right)(2k^-P^++mM)S^\perp. \tag{C10}$$

As in the cases for G_2 and $\tilde{G}_2$, k^- in this numerator is replaced by the expression

$$k^-=\frac{M^2}{2P^+}-\frac{[(P-k)^2-\lambda^2]}{2(P^+-k^+)}-\frac{(k_\perp^2+\lambda^2)}{2(P^+-k^+)}, \tag{C11}$$

and the second term cancels the propagator in the denominator of Eq. (C2). Thus, two types of k^- integrals appear in the expression for $g_T(x)$,

$$g_T(x)=\frac{ig^2}{16\pi^4}\frac{(x+\frac{m}{M})}{(1-x)}\int d^2k_\perp[M(M+m)(1-x)-k_\perp^2-\lambda^2]\times\int\frac{dk^-}{(k^2-m^2+i\epsilon)^2[(P-k)^2-\lambda^2+i\epsilon]} -\frac{ig^2}{16\pi^4}\frac{(x+\frac{m}{M})}{(1-x)})\int d^2k_\perp\int\frac{dk^-}{(k^2-m^2+i\epsilon)^2}. \tag{C12}$$

As Eq. (22) shows, the energy integral in the second line of the above equation is the origin of the δ-function.

The full expression for $g_T(x)$ is obtained as follows by using a transverse momentum cutoff, $\Lambda_\perp$:

$$g_T(x)=-\frac{g^2}{16\pi^2}\left(x+\frac{m}{M}\right)\left\{\frac{[M(M+m)(1-x)-\lambda^2+\omega]}{(k_\perp^2+\omega)}+\ln(k_\perp^2+\omega)\right\}_{k_\perp^2=0}^{\Lambda_\perp^2}+\frac{g^2}{16\pi^2}\frac{(x+\frac{m}{M})}{(1-x)})\times\ln\left(\frac{\Lambda_\perp^2+m^2}{m^2}\right)\delta(x), \tag{C13}$$

where ω is given by

$$\omega=-x(1-x)M^2+(1-x)m^2+x\lambda^2. \tag{C14}$$

APPENDIX D: $g_1(x)$ IN SDM

$g_1(x)$ is obtained by using $\gamma^\mu=\gamma^+$ in the parametrization given by Eq. (15),

$$\int\frac{d\lambda}{2\pi}e^{i\lambda x}\langle P,S|\bar{q}(0)\gamma^+\gamma_5 q(\lambda n)|P,S\rangle = 2g_1(x)S^+. \tag{D1}$$

The left-hand side of Eq. (D1) is written using SDM,

$$g_1(x)S^+ = \frac{ig^2}{2}\int\frac{d^4k}{(2\pi)^4}\delta(k^+-xP^+)\bar{u}(p)\times\frac{(\not{k}+m)}{(k^2-m^2+i\epsilon)}\gamma^+\gamma_5\frac{(\not{k}+m)}{(k^2-m^2+i\epsilon)}u(p)\times\frac{1}{[(p-k)^2-\lambda^2+i\epsilon]}. \tag{D2}$$

The numerator of the integrand in Eq. (D2) is calculated using the identities given by Eqs. (C3)–(C9),

$$\bar{u}(p)(\not{k}+m)\gamma^{+}\gamma_5(\not{k}+m)u(p) = -4k^{+2}S^{-} - [2k_\perp^2 - 2m^2 - 4mMx]S^{+} = 2[(m+xM)^2 - k_\perp^2]S^{+}. \quad \text{(D3)}$$

The following expression is obtained for $g_1(x)$ using a transverse momentum cutoff, $\Lambda_\perp$:

$$g_1(x) = -\frac{g^2}{16\pi^2}(1-x)\left\{\frac{[\omega+(m+xM)^2]}{k_\perp^2+\omega} + \ln(k_\perp^2+\omega)\right\}\Bigg|_{k_\perp^2=0}^{\Lambda_\perp^2}. \quad \text{(D4)}$$

Similar to other twist-2 PDFs, the numerator in Eq. (D3) does not have a term involving a k^{-}, and therefore, the cancellation of the propagator which leads to the $\delta(x)$ contribution does not occur for $g_1(x)$.

APPENDIX E: $g_2(x)$ IN SDM

$g_2(x)$ is obtained as follows by using Eqs. (D4) and (C13) in the relation $g_T(x) = g_1(x) + g_2(x)$:

$$g_2(x) = \frac{g^2}{16\pi^2}\left\{2\omega - \frac{m}{M}[(M+m)^2-\lambda^2] + (m+xM)^2\right\} \times \frac{(1-x)}{(k_\perp^2+\omega)}\Bigg|_{k_\perp^2=0}^{\Lambda_\perp^2} + \frac{g^2}{16\pi^2}\left(2x+\frac{m}{M}-1\right)\ln(k_\perp^2+\omega)\Bigg|_{k_\perp^2=0}^{\Lambda_\perp^2} + \frac{g^2}{16\pi^2}\frac{(x+\frac{m}{M})}{(1-x)}\ln\left(\frac{\Lambda_\perp^2+m^2}{m^2}\right)\delta(x), \quad \text{(E1)}$$

where the last term is called $g_{2,\delta}(x)$ in Eq. (24).

[1] D. Müller, D. Robaschik, B. Geyer, F. M. Dittes, and J. Horejsi, Fortschr. Phys. **42**, 101 (1994).
[2] A. V. Radyushkin, Phys. Lett. B **380**, 417 (1996).
[3] A. V. Radyushkin, Phys. Lett. B **385**, 333 (1996).
[4] X. D. Ji, Phys. Rev. D **55**, 7114 (1997).
[5] J. C. Collins and A. Freund, Phys. Rev. D **59**, 074009 (1999).
[6] M. Burkardt, Phys. Rev. D **62**, 071503 (2000); **66**, 119903 (E) (2002).
[7] M. Diehl, Eur. Phys. J. C **25**, 223 (2002); **31**, 277(E) (2003).
[8] M. Burkardt, Int. J. Mod. Phys. A **18**, 173 (2003).
[9] R. L. Jaffe, arXiv:hep-ph/9602236.
[10] S. Weinberg, Phys. Rev. **150**, 1313 (1966).
[11] J. D. Bjorken, Phys. Rev. **179**, 1547 (1969).
[12] M. Burkardt, Phys. Rev. D **88**, 114502 (2013).
[13] I. V. Anikin, B. Pire, and O. V. Teryaev, Phys. Rev. D **62**, 071501 (2000).
[14] I. V. Anikin, D. Binosi, R. Medrano, S. Noguera, and V. Vento, Eur. Phys. J. A **14**, 95 (2002).
[15] X. D. Ji, Phys. Rev. Lett. **78**, 610 (1997).
[16] M. Penttinen, M. V. Polyakov, A. G. Shuvaev, and M. Strikman, Phys. Lett. B **491**, 96 (2000).
[17] A. V. Belitsky and D. Müller, Nucl. Phys. **B589**, 611 (2000).
[18] N. Kivel, M. V. Polyakov, A. Schäfer, and O. V. Teryaev, Phys. Lett. B **497**, 73 (2001).
[19] A. V. Radyushkin and C. Weiss, Phys. Lett. B **493**, 332 (2000).
[20] N. Kivel and M. V. Polyakov, Nucl. Phys. **B600**, 334 (2001).
[21] A. V. Radyushkin and C. Weiss, Phys. Rev. D **63**, 114012 (2001).
[22] A. V. Belitsky, D. Müller, A. Kirchner, and A. Schäfer, Phys. Rev. D **64**, 116002 (2001).
[23] N. Kivel, M. V. Polyakov, and M. Vanderhaeghen, Phys. Rev. D **63**, 114014 (2001).
[24] I. V. Anikin and O. V. Teryaev, Phys. Lett. B **509**, 95 (2001).
[25] A. V. Belitsky, A. Kirchner, D. Müller, and A. Schäfer, Phys. Lett. B **510**, 117 (2001).
[26] N. Kivel and L. Mankiewicz, Eur. Phys. J. C **21**, 621 (2001).
[27] A. V. Belitsky, D. Müller, and A. Kirchner, Nucl. Phys. **B629**, 323 (2002).
[28] D. V. Kiptily and M. V. Polyakov, Eur. Phys. J. C **37**, 105 (2004).
[29] N. Kivel and L. Mankiewicz, Nucl. Phys. **B672**, 357 (2003).
[30] A. Freund, Phys. Rev. D **68**, 096006 (2003).
[31] S. Wandzura and F. Wilczek, Phys. Lett. **72B**, 195 (1977).
[32] J. C. Collins, D. E. Soper, and G. F. Sterman, Adv. Ser. Dir. High Energy Phys. **5**, 1 (1989).
[33] F. Aslan, M. Burkardt, C. Lorcé, A. Metz, and B. Pasquini, Phys. Rev. D **98**, 014038 (2018).
[34] S. Meissner, A. Metz, and M. Schlegel, J. High Energy Phys. 08 (2009) 056.
[35] S. V. Ivanov, G. P. Korchemsky, and A. V. Radyushkin, Yad. Fiz. **44**, 230 (1986) [Sov. J. Nucl. Phys. **44**, 145 (1986)].
[36] R. L. Jaffe and X. D. Ji, Phys. Rev. D **43**, 724 (1991).
[37] V. N. Gribov and L. N. Lipatov, Yad. Fiz. **15**, 781 (1972) [Sov. J. Nucl. Phys. **15**, 438 (1972)].
[38] L. N. Lipatov, Yad. Fiz. **20**, 181 (1974) [Sov. J. Nucl. Phys. **20**, 94 (1975)].
[39] G. Altarelli and G. Parisi, Nucl. Phys. **B126**, 298 (1977).
[40] Y. L. Dokshitzer, Zh. Eksp. Teor. Fiz. **73**, 1216 (1977) [Sov. Phys. JETP **46**, 641 (1977)].
[41] A. V. Efremov and A. V. Radyushkin, Teor. Mat. Fiz. **42**, 147 (1980) [Theor. Math. Phys. **42**, 97 (1980)].
[42] G. P. Lepage and S. J. Brodsky, Phys. Rev. D **22**, 2157 (1980).
[43] J. C. Collins and D. E. Soper, Nucl. Phys. **B194**, 445 (1982).
[44] R. L. Jaffe and X. D. Ji, Nucl. Phys. **B375**, 527 (1992).
[45] T. M. Yan, Phys. Rev. D **7**, 1780 (1973).
[46] X. Ji, Phys. Rev. Lett. **110**, 262002 (2013).

[47] X. Ji, Sci. China Phys. Mech. Astron. **57**, 1407 (2014).
[48] X. Xiong, X. Ji, J. H. Zhang, and Y. Zhao, Phys. Rev. D **90**, 014051 (2014).
[49] I. W. Stewart and Y. Zhao, Phys. Rev. D **97**, 054512 (2018).
[50] T. Izubuchi, X. Ji, L. Jin, I. W. Stewart, and Y. Zhao, Phys. Rev. D **98**, 056004 (2018).
[51] A. Harindranath and W. M. Zhang, Phys. Lett. B **408**, 347 (1997).
[52] M. Burkardt and Y. Koike, Nucl. Phys. **B632**, 311 (2002).
[53] M. Wakamatsu and Y. Ohnishi, Phys. Rev. D **67**, 114011 (2003).
[54] Y. Ohnishi and M. Wakamatsu, Phys. Rev. D **69**, 114002 (2004).
[55] A. V. Efremov and P. Schweitzer, J. High Energy Phys. 08 (2003) 006.
[56] P. Schweitzer, Phys. Rev. D **67**, 114010 (2003).
[57] H. Burkhardt and W. N. Cottingham, Ann. Phys. (N.Y.) **56**, 453 (1970).
[58] L. Theussl, S. Noguera, and V. Vento, Eur. Phys. J. A **20**, 483 (2004).
[59] P. D. Mannheim, P. Lowdon, and S. J. Brodsky, Phys. Lett. B **797**, 134916 (2019).
[60] J. Collins, arXiv:1801.03960.
[61] M. Burkardt, Phys. Rev. D **47**, 4628 (1993).
[62] F. P. Aslan and M. Burkardt (to be published).